

<https://doi.org/10.11646/mesozoic.1.3.19>

<http://zoobank.org/urn:lsid:zoobank.org:pub:19EAE762-6681-4014-9ED2-134183957123>

## Temporal scaling of carbon emission accumulations and rates of the Meso-Cenozoic hyperthermal events: implication to the Anthropocene global warming


XIU-MIAN HU<sup>1,\*</sup>, JING-XIN JIANG<sup>1</sup>, YUAN CAI<sup>1</sup>, ZHONG HAN<sup>2</sup> & YI-WEI XU<sup>1,3</sup>

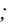
<sup>1</sup>State Key Laboratory of Mineral Deposit Research, School of Earth Sciences and Engineering, Nanjing University, Nanjing 210023, China

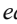
<sup>2</sup>State Key Laboratory of Oil and Gas Reservoir Geology and Exploitation, Institute of Sedimentary Geology, Chengdu University of Technology, Chengdu 610059, China

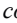
<sup>3</sup>State Key Laboratory of Paleobiology and Stratigraphy, Nanjing Institute of Geology and Palaeontology, Chinese Academy of Sciences, Nanjing 210008, China

✉ [huxm@nju.edu.cn](mailto:huxm@nju.edu.cn);  <https://orcid.org/0000-0002-5401-8682>

✉ [jjxcug24@163.com](mailto:jjxcug24@163.com);  <https://orcid.org/0009-0004-2217-2118>

✉ [cyuan\\_c@139.com](mailto:cyuan_c@139.com);  <https://orcid.org/0009-0009-3448-2558>

✉ [hanzhong19@cdut.edu.cn](mailto:hanzhong19@cdut.edu.cn);  <https://orcid.org/0000-0002-8690-454X>

✉ [kongjuzixing@126.com](mailto:kongjuzixing@126.com);  <https://orcid.org/0000-0002-3387-7453>

\*Corresponding author

### Abstract

Anthropocene global warming is largely associated with fossil fuel carbon emissions. Temporal scaling provides a way to place current carbon emissions on a geological scale. The scaling of carbon emissions at the onset of hyperthermal events suggests that we might anticipate higher carbon emission rates over longer time scales than what we currently observe in the Anthropocene. However, this inference is uncertain due to limited data concerning the accumulations and time intervals of carbon emissions of Meso-Cenozoic hyperthermal events. While on the long-time hyperthermal-event scales of several to hundreds of kiloyears, modern carbon accumulations and emission rates are 9 times greater than those of the hyperthermal-event emissions. The present-day carbon release can be effectively compared to the onset of hyperthermal events through temporal scaling. If current carbon emission trends persist, we may reach the carbon emission thresholds for hyperthermal events in one to three hundred years, getting an intensified hydrological cycle, enhanced continental weathering and ocean acidification. And if the situation gets worse, we may reach the upper limit of the carbon emission threshold for hyperthermal events (e.g., Permian-Triassic Boundary event, PTB) with a biotic mass extinction over four to thirteen hundred years. This study offers new insights into current carbon emissions from a temporal scale perspective, enhancing our understanding of contemporary climate change.

**Keywords:** time scaling, global warming, hyperthermal events, carbon emission, climate change

### Introduction

Global warming, the phenomenon of increasing average surface temperatures on Earth over the past one to two centuries, is suggested by a series of observations on various weather phenomena and their influence on climate (Harvey, 2000). Human activities since at least the beginning of the Industrial Revolution had a growing influence over the pace and extent of present-day climate change (Steffen *et al.*, 2011; Lewis & Maslin, 2015; Ruddiman *et al.*, 2015). The modern global carbon budget indicates that carbon release from anthropogenic activities now exceeds 10 petagrams (Pg) per year, primarily driven by fossil fuel carbon emissions, with a rate that is four times higher than that of the mid-20th century (Fig. 1; Friedlingstein *et al.*, 2023). People can't help but ask: How hot will the greenhouse world be? (Kerr, 2005). One way to appreciate the rates and process of current carbon release to the Earth's system is to compare present-day emissions to those in Earth's history.

Past climates inform our future (Tierney *et al.*, 2020). Earth's climate has changed over almost every conceivable timescale since the beginning of geologic time. Among them, periods characterized by rapid global warming (greater than 2–4 °C), a quick onset (1–100 kyr), and a relatively short total duration (no more than a few million years), are defined as “hyperthermal event” (Svensen, 2012; Foster *et al.*, 2018; Hu *et al.*,

2020). These hyperthermal events, particularly those that occurred in the Meso-Cenozoic, such as the Permian-Triassic Boundary event (PTB, 252 Ma), the End-Triassic Event (TJB, ~201 Ma), the early Toarcian Oceanic Anoxic Event (TOAE, ~183 Ma), the Cretaceous Oceanic Anoxic Event (OAE1a, ~120 Ma, OAE2, ~94 Ma) and the Paleocene-Eocene Thermal Maximum (PETM, ~56 Ma), had profound ramifications on climate, environment, ecology, and biodiversity, and bear similarities to the ongoing changes we are currently experiencing (Foster *et al.*, 2018; Hu *et al.*, 2020; He *et al.*, 2023; Shen *et al.*, 2024). Therefore, a comprehensive understanding of hyperthermal events throughout the Earth's history is crucial for gaining insights into and addressing present-day global warming. This study aims to place our current global warming in the context of rapid climate change in the Meso-Cenozoic Era using the method of "temporal scaling", offering insights into future climate change.

## Material and methods

In this study, we collected and compiled data of carbon accumulation and rates of the onset of representative Meso-Cenozoic hyperthermal events (PTB, TJB, TOAE, OAE1a, OAE2 and PETM) at different time scales, which are mainly sourced from modeling studies (Tables 1, 2). Carbon accumulations are generally estimated from the masses of carbon required to explain differences in carbon isotopic excursion. Rates of accumulation can be calculated by dividing an estimate of total accumulation with an estimate for the corresponding interval. But it should be noted that extracting information from the literature is complicated when authors fail to match accumulations, intervals, and rates explicitly. In this situation, we calculate carbon emission rates by ranking and combining reported carbon emission accumulations with their duration. The modern carbon emission data are based on the Global Carbon Budget and are known for the years 1959 to 2021 (<https://co2.earth/>; Friedlingstein *et al.*, 2023), a time series spanning 63 successive years (Fig. 1).

Temporal scaling is the quantitative relationship of differences and rates of geological processes in geological history to their associated time intervals they represent (ratio = difference/time interval or rate/time interval; Kukal, 1990). Temporal scaling is often studied on log-difference-interval (LDI) and log-rate-interval (LRI) graphs (Gingerich, 2019). The distribution of the variable data of geological events on the logarithm axis can provide us with the judgment conditions of whether the rate is independent or dependent on the time scale, so as to provide us with the basis of whether

the geological processes of different time scales can be compared. When the slope of the data on the LDI plot approaches 1.0 and the slope on the LRI plot approaches 0, the geological event can be judged as a directional process, and the difference increases with the increase of time interval; when the slope of data on LDI and LRI plots approaches 0.5, the geological event is a random process, and the difference shows direction reversal or inclusion stagnation in the course of time; when the slope of the data on the LDI plot approaches 0 and the slope on the LRI plot approaches -1.0, this geological event is a stationary process, and the difference is a static state with no net change (Gingerich, 1983, 1993, 2019, 2021). Therefore, when geological events appear as directional processes, their rates are independent of time intervals and can be compared on a wide range of time scales, and then the differences or rates on different time scales can be predicted by interpolation or extrapolation (Gingerich, 2021). The geological events of random or stationary processes are dependent on the time scale and need to be restricted to a time scale for comparison. This study calculated the carbon accumulation differences and rates at all scales of each hyperthermal event with full samples and plotted them on LDI and LRI for comparison and research.

## Results

### *Carbon release rates of Meso-Cenozoic hyperthermal events*

This study compares present-day's carbon emissions with those recorded throughout Earth's history, to better understand the rates and processes of current carbon release into the Earth's system. Further, we attempt to determine the comparability of carbon accumulation from these geological processes on different time scales and try to predict development trends of carbon emissions in the future.

The PTB event (~252 Ma) represents the largest warming (~8–10 °C) amplitude in the Phanerozoic (Joachimski *et al.*, 2012; Sun *et al.*, 2012). During the PTB, bulk carbon isotopes underwent at least three cycles of negative excursion and recovery, including a significant negative carbon isotopic excursion (CIE) exceeding 7‰ (Cao *et al.*, 2009). It has been estimated that 3,900 to 105,600 Pg C carbon were released during the onset of the PTB spanning about 1,000 to 75,000 years (Schneebeil-Hermann *et al.*, 2013; Clarkson *et al.*, 2015; Cui *et al.*, 2013, 2021; Jurikova *et al.*, 2021; Wu *et al.*, 2021; Shen *et al.*, 2022), on the time scale of which the corresponding rate is 1.4 to 3.9 (the maximum is 24) Pg C/year.

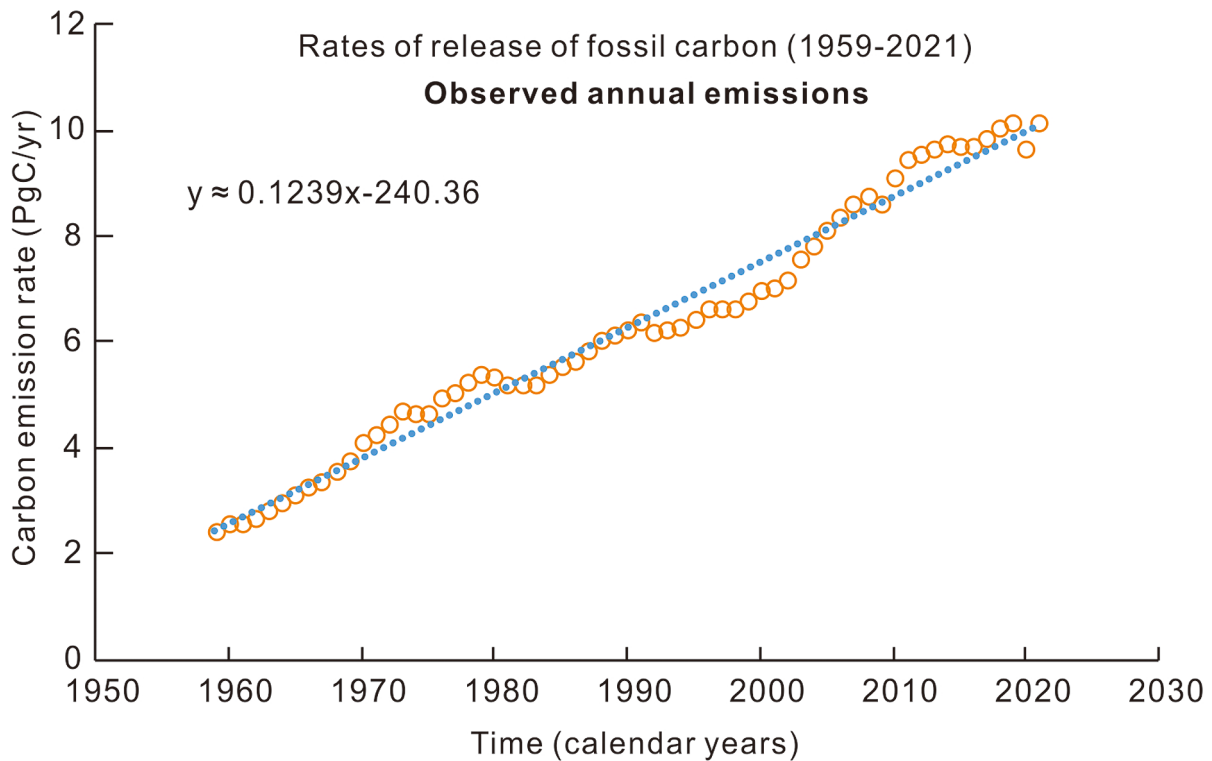


**FIGURE 1.** Global annual fuel fossil carbon emissions and carbon emission rates for the years 1959 through 2021 (data from Friedlingstein *et al.*, 2023). Emission rates are now nearly 10 Pg C/year on a time scale of 1 year. Line fit to the points shows the long-term trend.

The TJB event occurred at the end-Triassic (~201 Ma), with 3–4 °C temperature rising and ~1.5% negative CIE (Schaller *et al.*, 2011; Blackburn *et al.*, 2013). Carbon emissions during the onset of the TJB have been estimated to reach 2,000 to 14,000 Pg C, over an interval of 10,000 to 110,000 years, for a rate of 0.08 to 0.65 Pg C/year (Beerling & Berner, 2002; Ruhl *et al.*, 2010, 2011, 2020; Heimdal *et al.*, 2020).

The TOAE (~183 Ma) resulted in a warming of 7–10 °C in the northern middle latitudes and is characterized by a CIE magnitude of 3–7‰ (Kemp *et al.*, 2005; Suan *et al.*, 2008; Jenkyns, 2010). During the TOAE, an estimated 6,000 to 40,000 Pg C accumulated over a duration of 150,000 to 220,000 years, yielding an average rate of 0.04 to 0.27 Pg C per year (Beerling & Brentnall, 2007, 2008; Brazier *et al.*, 2015; Them II *et al.*, 2017).

The OAE1a occurred at the early Aptian in the Early Cretaceous (~120 Ma) with a warming of 5–6 °C (Mutterlose *et al.*, 2010; Naafs & Pancost, 2016), and with an extremely negative CIE and then a 3–7‰ positive excursion (Menegatti *et al.*, 1998). Carbon emissions during the onset of the OAE1a have been estimated to reach 1,763 to 59,860 Pg C, over an interval of 41,000 to 485,000 years, for a rate of 0.003 to 1.28 Pg C/year (Li *et al.*, 2008; Scott, 2016; Adloffs *et al.*, 2020; Beil *et al.*, 2020; Charbonnier *et al.*, 2023).

The OAE2 occurred at the end of the Cenomanian (~94 Ma), with a warming of 2–3 °C at low latitude and 7–10°C at high latitude (Jenkyns *et al.*, 2004; Foster *et al.*, 2007; Huber *et al.*, 2018). There was overall a greater than 2‰ positive CIE, before which appeared a weak negative excursion in an expanded section (Jenkyns *et al.*, 2010; Li *et al.*, 2017). It has been estimated that 3,000 to 32,700 Pg C carbon were released during the onset of the OAE2 spanning about 7,000 to 500,000 years (Kuroda *et al.*, 2007; Clarkson *et al.*, 2018; Beil *et al.*, 2020), on the time scale of which the corresponding rate is 0.07 to 4.67 Pg C/year.

The PETM occurred at the boundary of the Paleocene and Eocene (~56 Ma) and was marked by a 3–7‰ negative CIE, during which the temperature rose 5–8 °C (Kennett & Stott, 1991; Zachos *et al.*, 2001; McInerney & Wing, 2011). The PETM was caused by the injection of 3,000–13,000 Pg C during the onset spanning about 1,500 to 25,000 years, for a rate of 0.5–2.0 Pg C/year (Zeebe *et al.*, 2009, 2016; Cui *et al.*, 2011; Bowen *et al.*, 2015; Gutjahr *et al.*, 2017).

Overall, the carbon emission rate of Meso-Cenozoic hyperthermal events ranges from 0.004–5.28 Pg C/year (only one extreme value exceeds 6 Pg C/year; Tables 1, 2). For comparison, the average present-day fuel fossil carbon release rate is 6 Pg C/year over a one-year timescale and

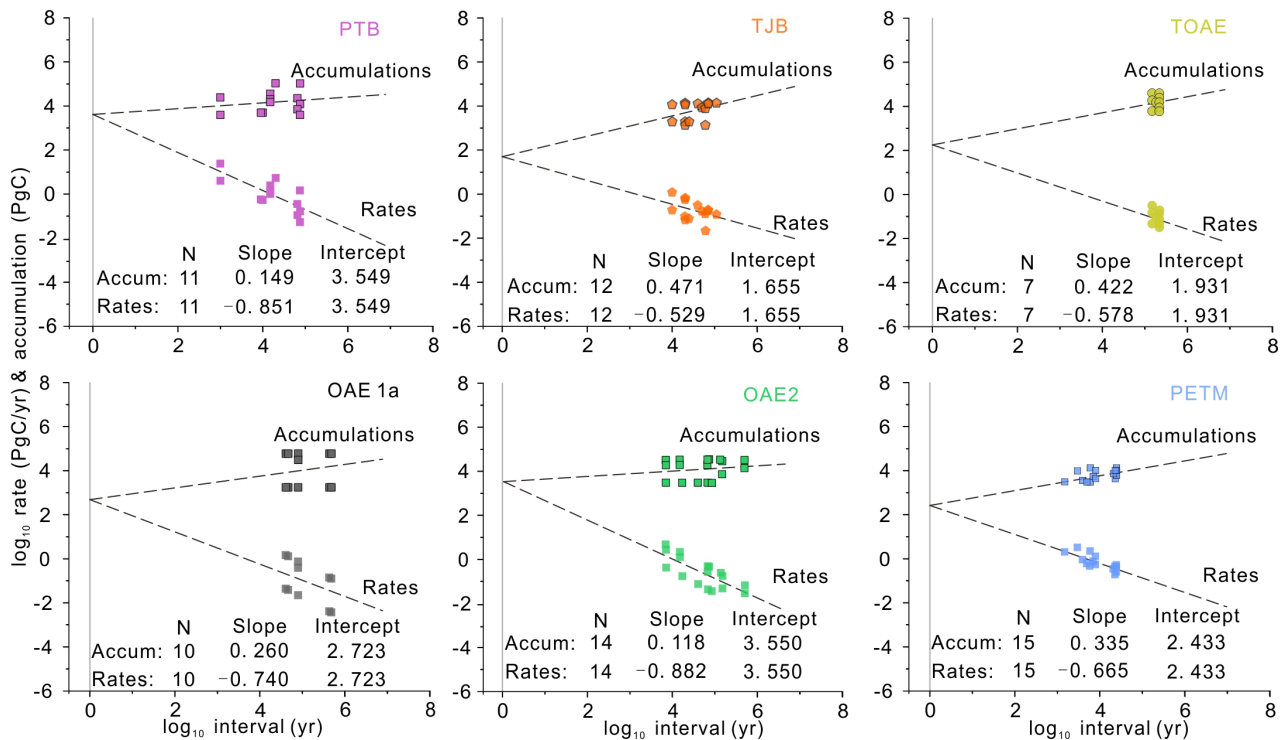


**FIGURE 2.** Carbon accumulations and accumulation rates estimated for the onset of hyperthermal events. The contoured icons represent the carbon accumulation during the onset of the hyperthermal events, whereas the un-contoured icons indicate the rates of carbon accumulation. Dotted lines are fit to accumulations and rates of hyperthermal events for corresponding time intervals, pointing to a common short-term hyperthermal-event rate (intercepts) on a time scale of one year.

has been nearly 10 Pg C/year in 2021 (Fig. 1; Friedlingstein *et al.*, 2023), which, at first glance, surpasses the rates of all Meso-Cenozoic hyperthermal events rates by a factor of at least 1~2. However, this comparison was conducted on different time scales, which may result in a statistical deception.

#### Contextualizing modern carbon emissions and rates within geological history

This study compares the rates of carbon emission today to those during the onset of the Meso-Cenozoic hyperthermal events in two ways: (1) projection of long-term hyperthermal events rates for comparison on an annual time scale and (2) projection of short-term modern rates for comparison on a hyperthermal events time scale.

Fig. 2 shows combined LDI-LRI plots for temporal scaling of onset accumulations and rates of hyperthermal events listed in Tables 1 and 2. Generally, the higher rates are those calculated on shorter time scales, and the lower rates are those calculated on longer time scales. The lines fit to hyperthermal-event rates have slopes of -0.851 (PTB), -0.529 (TJB), -0.578 (TOAE), -0.740 (OAE1a), -0.882 (OAE2) and -0.665 (PETM), and the lines fit to hyperthermal-event accumulations have slopes of 0.149 (PTB), 0.471 (TJB), 0.422 (TOAE), 0.260 (OAE1a),

0.118 (OAE2) and 0.335 (PETM). The slopes of accumulations and rates of hyperthermal events are close to the slope expected for a random geologic event (0.500 for accumulations and -0.500 for rates; Gingerich, 2021). The fitted lines of accumulations and rates have the same intercept, which corresponds to predicted hyperthermal event rates of  $10^{3.549} = 3539$  Pg C (PTB),  $10^{1.655} = 45$  Pg C (TJB),  $10^{1.931} = 85$  Pg C (TOAE),  $10^{2.723} = 528$  Pg C (OAE1a),  $10^{3.550} = 3548$  Pg C (OAE2) and  $10^{2.433} = 271$  Pg C (PETM) on a time scale of one year. Due to limited data on accumulation and rate estimates, as well as the failure to explicitly match accumulations, intervals, and rates, the extrapolated rate of carbon release during the hyperthermal event (ranging from 45 to 3,539 Pg C/year) over a one-year timescale is poorly constrained and may not be significantly greater than modern carbon emissions within the same timeframe.

Fig. 3 is a combined LDI-LRI plot for temporal scaling of the 1,953 modern carbon emissions and emission rates based on the 63 annual values from the Global Carbon Budget (Friedlingstein *et al.*, 2023). The 1,953 modern rates range from 2.417 to 10.132 Pg C/year (0.383 to 1.006 on  $\log_{10}$  scale), on a time scale or interval of 1 to 63 years. The temporal scaling slope of modern carbon emission rates is 0.028 (Fig. 3), closely aligning with the

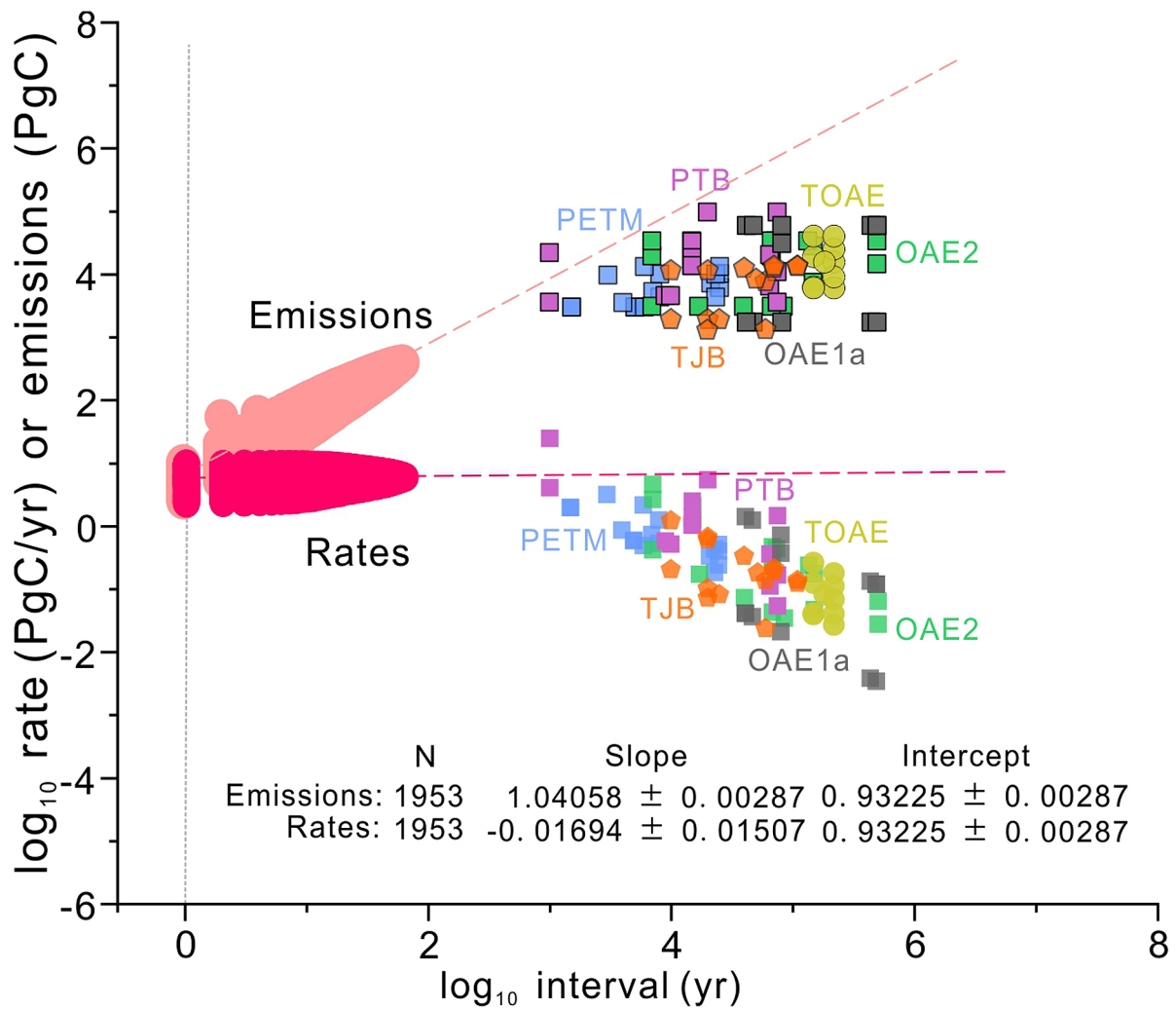


**FIGURE 3.** Carbon accumulations and accumulation rates estimated for the hyperthermal events compared to modern carbon accumulations (pale pink circles) and rates (rose pink circles). Modern carbon emission data are from Friedlingstein *et al.* (2023). The accumulations and rates data of hyperthermal events refer to Tables 1, 2.

**TABLE 1.** A summary of representative hyperthermal events in the Meso-Cenozoic (references refer to the Table 2).

Hyperthermal event	Age (Ma)	Onset duration (kyr)	Total duration (kyr)	CIE (%)	Global warming ( $\Delta^{\circ}\text{C}$ )	Onset carbon release (Pg C)	*Carbon emission rate (Pg C/year)
PTB	~252	1~75	>5000	5~7	8~10	3900~105600	1.4~3.9
TJB	~201	10~110	1200	~1.5	3~4	2000~14000	0.08~0.65
TOAE	~183	150~220	300	3~7	7~10 (mid-latitude)	6000~4000000	0.04~0.27
OAE1a	~120	41~485	1145	-	5~6	1763~59860	0.003~1.28
OAE2	~94	7~500	1322	-	2~3	3000~32700	0.07~4.67
PETM	~56	1.5~25	170~200	3~7	5~8	3000~13000	0.5~2.0

\*Carbon emission rates calculated by ranking and combining all reported carbon emission accumulations with their duration.

expected slope of 0 for a directional process, indicating that modern carbon emissions are neither stationary nor random. (Gingerich, 2021). Both accumulation

and rate have the same intercept of 0.932, which yields a predicted modern rate of  $10^{0.948} = 8.551$  Pg C/year. Due to modern carbon emissions being a directional

**TABLE 2** Published estimates for the time interval, carbon accumulation, and carbon accumulation rate of the onset of hyperthermal events.

Hyperthermal event	Time interval (year)	Accumulation (Pg C)	Rate (Pg C/yr)	Log10 interval	Log10 accumulation	Log10 rate	Source
PTB	1000	24000	24.000	3.000	4.380	1.380	Clarkson <i>et al.</i> , 2015
PTB	9000	5000	0.556	3.954	3.699	-0.255	Shen <i>et al.</i> , 2022
PTB	10000	5000	0.500	4.000	3.699	-0.301	Shen <i>et al.</i> , 2022
PTB	15000	15000	1.000	4.176	4.176	0.000	Hermann <i>et al.</i> , 2013
PTB	15000	20000	1.333	4.176	4.301	0.125	Hermann <i>et al.</i> , 2013
PTB	15000	36000	2.400	4.176	4.556	0.380	Cui <i>et al.</i> , 2021
PTB	20000	105600	5.280	4.301	5.024	0.723	Jurikova <i>et al.</i> , 2021
PTB	65000	7000	0.108	4.813	3.845	-0.968	Cui <i>et al.</i> , 2013
PTB	65000	22400	0.345	4.813	4.350	-0.463	Cui <i>et al.</i> , 2013
PTB	75000	3900	0.052	4.875	3.591	-1.284	Wu <i>et al.</i> , 2021
PTB	75000	12000	0.160	4.875	4.079	-0.796	Wu <i>et al.</i> , 2021
TJB	10000	12000	1.200	4.000	4.079	0.079	Ruhl <i>et al.</i> 2011
TJB	20000	1400	0.070	4.301	3.146	-1.155	Bachan & Payne, 2016
TJB	20000	2000	0.100	4.301	3.301	-1.000	Ruhl <i>et al.</i> , 2010
TJB	20000	12000	0.600	4.301	4.079	-0.222	Ruhl <i>et al.</i> , 2011
TJB	20000	13000	0.650	4.301	4.114	-0.187	Scaller <i>et al.</i> , 2011
TJB	25000	2000	0.080	4.398	3.301	-1.097	Ruhl <i>et al.</i> , 2020
TJB	40000	13000	0.325	4.602	4.114	-0.488	Ruhl <i>et al.</i> , 2010
TJB	50000	8800	0.176	4.699	3.944	-0.754	Heimdal <i>et al.</i> , 2020
TJB	60000	1400	0.023	4.778	3.146	-1.632	Yager <i>et al.</i> , 2017
TJB	70000	13000	0.186	4.845	4.114	-0.731	Beerling & Berner, 2002
TJB	70000	14000	0.200	4.845	4.146	-0.699	Beerling & Berner, 2002
TJB	110000	14000	0.127	5.041	4.146	-0.895	Yager <i>et al.</i> , 2017
TOAE	150000	6220	0.041	5.176	3.794	-1.382	Them II <i>et al.</i> , 2017
TOAE	150000	18869	0.126	5.176	4.276	-0.900	Them II <i>et al.</i> , 2017
TOAE	150000	40000	0.267	5.176	4.602	-0.574	Brazier <i>et al.</i> , 2015
TOAE	220000	6000	0.027	5.342	3.778	-1.564	Beerling & Brentnall, 2008
TOAE	220000	9000	0.041	5.342	3.954	-1.388	Beerling & Brentnall, 2008
TOAE	220000	15340	0.070	5.342	4.186	-1.157	Beerling & Brentnall, 2007
TOAE	220000	24750	0.113	5.342	4.394	-0.949	Beerling & Brentnall, 2007
OAE1a	41000	1763	0.043	4.613	3.246	-1.367	Li <i>et al.</i> , 2008; Adloffs <i>et al.</i> , 2020
OAE1a	41000	59860	1.460	4.613	4.777	0.164	Li <i>et al.</i> , 2008; Adloffs <i>et al.</i> , 2020
OAE1a	46700	1763	0.038	4.669	3.246	-1.423	Malinerno <i>et al.</i> , 2010

.....continued on the next page

TABLE 2 (Continued)

Hyperthermal event	Time interval (year)	Accumulation (Pg C)	Rate (Pg C/yr)	Log10 interval	Log10 accumulation	Log10 rate	Source
OAE1a	46700	59860	1.282	4.669	4.777	0.108	Malinerno <i>et al.</i> , 2010
OAE1a	80000	1763	0.022	4.903	3.246	-1.657	Scott, 2016
OAE1a	80000	59860	0.748	4.903	4.777	-0.126	Scott, 2016
OAE1a	434000	1763	0.004	5.637	3.246	-2.391	Beil <i>et al.</i> , 2020
OAE1a	434000	59860	0.138	5.637	4.777	-0.860	Beil <i>et al.</i> , 2020
OAE1a	485000	1763	0.004	5.686	3.246	-2.439	Charbonnier <i>et al.</i> , 2023
OAE1a	485000	59860	0.123	5.686	4.777	-0.909	Charbonnier <i>et al.</i> , 2023
OAE2	7000	19000	2.714	3.845	4.279	0.434	Kuroda <i>et al.</i> , 2007
OAE2	7000	32700	4.671	3.845	4.515	0.669	Kuroda <i>et al.</i> , 2007
OAE2	15000	19000	1.267	4.176	4.279	0.103	Kuroda <i>et al.</i> , 2007
OAE2	15000	32700	2.180	4.176	4.515	0.338	Kuroda <i>et al.</i> , 2007
OAE2	17000	3000	0.176	4.230	3.477	-0.753	Gang <i>et al.</i> , 2019
OAE2	40000	3000	0.075	4.602	3.477	-1.125	Papadomanolaki <i>et al.</i> , 2020
OAE2	68000	3000	0.044	4.833	3.477	-1.355	Beil <i>et al.</i> , 2020
OAE2	68000	32700	0.481	4.833	4.515	-0.318	Beil <i>et al.</i> , 2020
OAE2	73000	32700	0.448	4.863	4.515	-0.349	Gang <i>et al.</i> , 2019
OAE2	85000	3000	0.035	4.929	3.477	-1.452	Li <i>et al.</i> , 2017
OAE2	135000	32700	0.242	5.130	4.515	-0.616	Li <i>et al.</i> , 2017
OAE2	150000	7200	0.048	5.176	3.857	-1.319	Clarkson <i>et al.</i> , 2018
OAE2	150000	27000	0.180	5.176	4.431	-0.745	Clarkson <i>et al.</i> , 2018
OAE2	500000	14160	0.028	5.699	4.151	-1.548	Joo <i>et al.</i> , 2020
PETM	1500	3000	2.000	3.176	3.477	0.301	Bowen <i>et al.</i> , 2015
PETM	3000	9660	3.220	3.477	3.985	0.508	Kirtl & Turner, 2018
PETM	4000	3500	0.875	3.602	3.544	-0.058	Zeebe <i>et al.</i> , 2016
PETM	5000	3000	0.600	3.699	3.477	-0.222	Zeebe <i>et al.</i> , 2009; Frieling <i>et al.</i> , 2016
PETM	6000	3000	0.500	3.778	3.477	-0.301	Li <i>et al.</i> , 2022
PETM	6000	13000	2.167	3.778	4.114	0.336	Li <i>et al.</i> , 2022
PETM	8000	4300	0.538	3.903	3.633	-0.270	McInerney & Wing, 2011
PETM	8000	10000	1.250	3.903	4.000	0.097	McInerney & Wing, 2011
PETM	21000	7126	0.339	4.322	3.853	-0.469	Cui <i>et al.</i> , 2011
PETM	23000	4300	0.187	4.362	3.633	-0.728	McInerney & Wing, 2011
PETM	23000	10000	0.435	4.362	4.000	-0.362	McInerney & Wing, 2011
PETM	25000	6141	0.246	4.398	3.788	-0.610	Gutjahr <i>et al.</i> , 2017
PETM	25000	10200	0.408	4.398	4.009	-0.389	Gutjahr <i>et al.</i> , 2017

process, the rate will also remain constant on the scale of hyperthermal events, *i.e.*, 1 to 500 millennia. Thus, on the same scale of time, the present-day carbon emission rate is significantly different and 9-time higher than the average rate of hyperthermal events of 0.945 Pg C/year on a hyperthermal-event time scale (Tables 1, 2). Fig. 3 shows this graphically by the vertical distance between the dashed double red line confidence interval and the contoured color icons. Extrapolation of modern emissions to a hyperthermal-event time scale yields a similar result, where modern emissions are again projected to be some 9 times greater than hyperthermal-event emissions (uncontoured color icons). Even so, the accumulations and rates of carbon emission of hyperthermal events fall near the extrapolation line of accumulation and rate of modern carbon emissions, indicating that present-day carbon release can be compared with the onset of hyperthermal events by temporal scaling.

#### Projecting Modern Carbon Emissions into the Future

The directional characteristics of modern carbon emissions recorded by successive 63-year observed data indicate that while emissions may fluctuate in the future, a steady increase will be observed in the annual rate of carbon added to the atmosphere (Fig. 1).

Where will the future go? As shown in Fig. 1, the carbon emission (y) per year (x) from 1959 to 2021 satisfies a linear equation fitting:  $y \approx 0.1239x - 240.36$ . A simple extrapolation carbon accumulation is shown in Fig. 4, in which the modern observed carbon

emissions are shown in red, and the inferred future carbon emission accumulations are shown in grey. From 1959 to 2021, total fossil fuel carbon emissions have reached 395 Pg C, a figure that falls short of the emissions associated with the onset of any hyperthermal events. However, projecting emissions forward in time, we may see carbon emission scenarios of hyperthermal events in the near future (as few as a hundred years). For example, we can expect to reach the estimated lower limit of the PETM carbon accumulation value of 3,000 Pg C in the year 2159, and we can expect to reach the upper limit of the PETM accumulation value of 13,000 Pg C in the year 2405. Overall, with the exception of the maximum estimated carbon emissions from the PTB event, we can theoretically expect to reach all other carbon emission scenarios from Meso-Cenozoic hyperthermal events within the next thousand years: 84 to 229 years for lower estimates and 383 to 1,337 years for upper estimates of carbon accumulation.

Hyperthermal events are further categorized into two types: positive carbon excursion hyperthermal event (PCHE, represented by OAE1a, OAE2) and negative carbon excursion hyperthermal event (NCHE, represented by PTB, TOAE and PETM), which correspond to different forms of carbon release from the Earth's inner system, and also show different responses in sedimentation, environment and ecology (Hu *et al.*, 2020). From the point of view of the lower limit of carbon emissions estimate, PCHEs and NCHEs can be bounded by 3,000 Pg C carbon emissions. This suggests that in the future, we

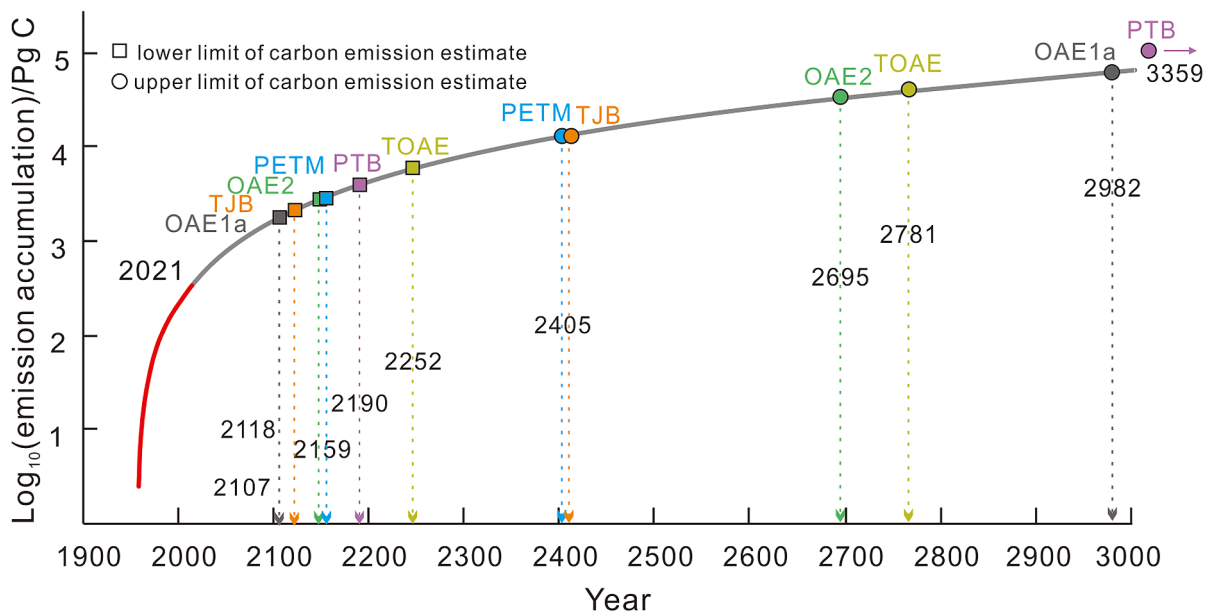


**FIGURE 4.** Model for carbon accumulation as the sum of carbon emissions, based on the steady increase in emissions and emission rates shown in Fig 1. Red line part represents annual accumulations from 1959 to 2021 and grey line part represents inferred future carbon emissions. Squares and circles represent the lower and upper limits of carbon emission estimate of Meso-Cenozoic hyperthermal events, respectively.



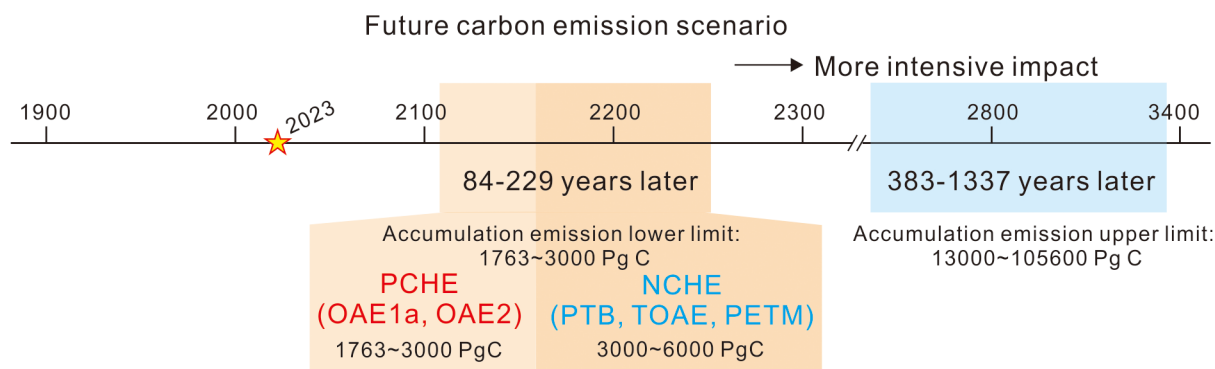


**FIGURE 5.** The scenarios of modern carbon emission accumulation align with the PCHE and NCHE onset in the future.

will first encounter PCHE-dominated system responses in 84 to 136 years, such as platform demise and ocean anoxia, followed by NCHE-dominated responses in 136 to 229 years, including an intensified hydrological cycle, enhanced continental weathering, and ocean acidification (Robinson *et al.*, 2017; Foster *et al.*, 2018; Hu *et al.*, 2020; He *et al.*, 2023). And if the situation gets worse, we may reach the upper limit of the carbon emission threshold for hyperthermal events like the PTB in 383 to 1,337 years (Fig. 5). While there is significant uncertainty in this comparison and inference, it offers valuable insights into our understanding of current global warming on the scale of hyperthermal events. In the future, it may be essential to consider various parameters, such as temperature, carbon isotopes, and background CO<sub>2</sub> levels, for a more detailed comparison to enhance this understanding.

## Conclusion

This study compares present-day carbon emissions to carbon accumulations from geological history using a temporal scaling method. The scaling of carbon accumulation rates at the onset of hyperthermal events suggests that we might expect higher carbon emission rates over longer time scales than what we currently observe in the short term. However, this inference is uncertain due to limited or mismatched data regarding the accumulations and time intervals of carbon emissions during hyperthermal events. While on the long-time hyperthermal-event scales of several to hundreds of kiloyears, modern carbon accumulations and emission rates are 9 times greater than hyperthermal-event emissions.

On the same scale of time, the accumulation and rate of carbon emissions during hyperthermal events fall near the extrapolation line of modern emissions, indicating that present-day carbon release can be effectively compared to the onset of hyperthermal events through temporal

scaling. If current carbon emission trends continue, we may reach the carbon emission threshold for PCHE-type hyperthermal events in 84 to 136 years, and for NCHE-type hyperthermal events in 136 to 229 years.

## Acknowledgements

Juan Li and Jiawei He are thanked for their assistance in data compilation. This work was supported by the National Natural Science Foundation of China (42488201) and is a contribution to the IGCP739. This paper is dedicated to our dear friend Dr Juan Li who spent her last moments logging the PETM interval in the Tibetan Himalayas.

## References

- Adloff, M., Greene, S.E., Parkinson, I.J., Naafs, B.D.A., Preston, W., Ridgwell, A., Lunt, D., Castro-Jimenez, J. & Monteiro, F.M. (2020) Unravelling the sources of carbon emissions at the onset of Oceanic Anoxic Event (OAE) 1a. *Earth and Planetary Science Letters*, 530, 115947. <https://doi.org/10.1016/j.epsl.2019.115947>
- Beerling, D.J. & Berner, R.A. (2002) Biogeochemical constraints on the Triassic–Jurassic boundary carbon cycle event. *Global Biogeochemical Cycles*, 16 (3), 10-1-10-13. <https://doi.org/10.1029/2001GB001637>
- Beerling, D.J. & Brentnall, S.J. (2007) Numerical evaluation of mechanisms driving Early Jurassic changes in global carbon cycling. *Geology*, 35 (3), 247–250. <https://doi.org/10.1130/G23416A.1>
- Beil, S., Kuhnt, W., Holbourn, A., Scholz, F., Oxmann, J., Wallmann, K., Lorenzen, J., Aquit, A. & Chellai, E.H. (2020) Cretaceous oceanic anoxic events prolonged by phosphorus cycle feedbacks. *Climate of the Past*, 16 (2), 757–782. <https://doi.org/10.5194/cp-16-757-2020>

- Blackburn, T.J., Olsen, P.E., Bowring, S.A., McLean, N.M., Kent, D.V., Puffer, J., Mchone, G., Rasbury, E. & Et-Touhami, M. (2013) Zircon U-Pb geochronology links the end-Triassic extinction with the Central Atlantic Magmatic Province. *Science*, 340 (6135), 941–945.  
<https://doi.org/10.1126/science.1234204>
- Bowen, G.J., Maibauer, B.J., Kraus, M. J., Röhl, U., Westerhold, T., Steimke, A., Gingerich, P., Wing, L. & Clyde, W.C. (2015) Two massive, rapid releases of carbon during the onset of the Palaeocene–Eocene thermal maximum. *Nature Geoscience*, 8 (1), 44–47.  
<https://doi.org/10.1038/ngeo2316>
- Brazier, J.M., Suan, G., Tacail, T., Simon, L., Martin, J.E., Mattioli, E. & Balter, V. (2015) Calcium isotope evidence for dramatic increase of continental weathering during the Toarcian oceanic anoxic event (Early Jurassic). *Earth and Planetary Science Letters*, 411, 164–176.  
<https://doi.org/10.1016/j.epsl.2014.12.023>
- Cao, C. & Zheng, Q. (2009) Geological event sequences of the Permian–Triassic transition recorded in the microfacies in Meishan section. *Science in China Series D: Earth Sciences*, 52 (10), 1529–1536.  
<https://doi.org/10.1007/s11430-009-0113-0>
- Charbonnier, G., Boulila, S., Spangenberg, J.E., Vermeulen, J. & Galbrun, B. (2023) Astrochronology of the Aptian stage and evidence for the chaotic orbital motion of Mercury. *Earth and Planetary Science Letters*, 610, 118104.  
<https://doi.org/10.1016/j.epsl.2023.118104>
- Clarkson, M.O., Kasemann, S.A., Wood, R.A., Lenton, T.M., Daines, S.J., Richoz, S., Ohnemueller, F., Meixner, A., Poulton, W. & Tipper, E.T. (2015) Ocean acidification and the Permo-Triassic mass extinction. *Science*, 348 (6231), 229–232.  
<https://doi.org/10.1126/science.aaa0193>
- Clarkson, M.O., Stirling, C.H., Jenkyns, H.C., Dickson, A.J., Porcelli, D., Moy, C.M., Pogge von Strandmann, P., Cooke, I. & Lenton, T.M. (2018) Uranium isotope evidence for two episodes of deoxygenation during Oceanic Anoxic Event 2. *Proceedings of the National Academy of Sciences*, 115 (12), 2918–2923.  
<https://doi.org/10.1073/pnas.1715278115>
- Cui, Y., Kump, L. R., Ridgwell, A. J., Charles, A. J., Junium, C.K., Diefendorf, A.F., Freeman, K., Urban, N. & Harding, I.C. (2011) Slow release of fossil carbon during the Palaeocene–Eocene Thermal Maximum. *Nature Geoscience*, 4 (7), 481–485.  
<https://doi.org/10.1038/ngeo1179>
- Cui, Y., Kump, L. R. & Ridgwell, A. (2013) Initial assessment of the carbon emission rate and climatic consequences during the end-Permian mass extinction. *Palaeogeography, Palaeoclimatology, Palaeoecology*, 389, 128–136.  
<https://doi.org/10.1016/j.palaeo.2013.03.020>
- Cui, Y., Li, M., Van Soelen, E.E., Peterse, F. & Kürschner, W.M. (2021) Massive and rapid predominantly volcanic CO<sub>2</sub> emission during the end-Permian mass extinction. *Proceedings of the National Academy of Sciences*, 118 (37), e2014701118.  
<https://doi.org/10.1073/pnas.2014701118>
- Foster, G.L., Hull, P., Lunt, D.J. & Zachos, J.C. (2018) Placing our current ‘hyperthermal’ in the context of rapid climate change in our geological past. *Philosophical Transactions of the Royal Society A: Mathematical, Physical and Engineering Sciences*, 376 (2130), 20170086.  
<http://dx.doi.org/10.1098/rsta.2017.0086>
- Friedlingstein, P., O’Sullivan, M., Jones, M.W., Andrew, R.M., Bakker, D. *et al.* (2023) Global Carbon Budget 2023. *Earth System Science Data*, 15, 5301–5369.  
<https://doi.org/10.5194/essd-15-5301-2023>
- Gingerich, P.D. (1983) Rates of evolution: effects of time and temporal scaling. *Science*, 222 (4620), 159–161.  
<https://doi.org/10.1126/science.222.4620.159>
- Gingerich, P.D. (1993) Quantification and comparison of evolutionary rates. *American Journal of Science*, 293A, 453–478.  
<https://doi.org/10.2475/ajs.293.a.453>
- Gingerich, P.D. (2019) Temporal scaling of carbon emission and accumulation rates: modern anthropogenic emissions compared to estimates of PETM onset accumulation. *Paleoceanography and Paleoclimatology*, 34 (3), 329–335.  
<https://doi.org/10.1029/2018PA003379>
- Gingerich, P.D. (2021) Rates of geological processes. *Earth-Science Reviews*, 220, 103723.  
<https://doi.org/10.1016/j.earscirev.2021.103723>
- Gutjahr, M., Ridgwell, A., Sexton, P.F., Anagnostou, E., Pearson, P.N., Pälike, H., Norris, R., Thomas, E. & Foster, G.L. (2017) Very large release of mostly volcanic carbon during the Palaeocene–Eocene Thermal Maximum. *Nature*, 548 (7669), 573–577.  
<https://doi.org/10.1038/nature23646>
- Harvey, L.D. (2000) Global warming (1<sup>st</sup> ed). *Routledge, London*. 376 pp.  
<https://doi.org/10.4324/9781315838779>
- Heimdal, T.H., Jones, M.T. & Svensen, H.H. (2020) Thermogenic carbon release from the Central Atlantic magmatic province caused major end-Triassic carbon cycle perturbations. *Proceedings of the National Academy of Sciences*, 117 (22), 11968–11974.  
<https://doi.org/10.1073/pnas.2005586117>
- He, T., Kemp, D.B., Li, J. & Ruhl, M. (2023) Paleoenvironmental changes across the Mesozoic–Paleogene hyperthermal events. *Global and Planetary Change*, 222, 104058.  
<https://doi.org/10.1016/j.gloplacha.2023.104058>
- Hu, X., Li, J., Han, Z. & Li, Y. (2020) Two types of hyperthermal events in the Mesozoic–Cenozoic: Environmental impacts, biotic effects, and driving mechanisms. *Science China Earth Sciences*, 63 (8), 1041–1058.  
<https://doi.org/10.1007/s11430-019-9604-4>

- Jenkyns, H.C. (2010) Geochemistry of oceanic anoxic events. *Geochemistry, Geophysics, Geosystems*, 11 (3), 1–30. <https://doi.org/10.1029/2009GC002788>
- Joachimski, M.M., Lai, X., Shen, S., Jiang, H., Luo, G., Chen, B., Chen, J. & Sun, Y. (2012) Climate warming in the latest Permian and the Permian–Triassic mass extinction. *Geology*, 40 (3), 195–198. <https://doi.org/10.1130/G32707.1>
- Jurikova, H., Gutjahr, M., Wallmann, K., Flögel, S., Liebetrau, V., Posenato, R., Angiolini, L., Garbelli, C., Brand, U., Wiedenbeck, M. & Eisenhauer, A. (2020) Permian–Triassic mass extinction pulses driven by major marine carbon cycle perturbations. *Nature Geoscience*, 13 (11), 745–750. <https://doi.org/10.1038/s41561-020-00646-4>
- Kemp, D.B., Coe, A.L., Cohen, A.S. & Schwark, L. (2005) Astronomical pacing of methane release in the Early Jurassic period. *Nature*, 437 (7057), 396–399. <https://doi.org/10.1038/nature04037>
- Kennett, J.P. & Stott, L.D. (1991) Abrupt deep-sea warming, palaeoceanographic changes and benthic extinctions at the end of the Palaeocene. *Nature*, 353 (6341), 225–229. <https://doi.org/10.1038/353225a0>
- Kerr, R.A. (2005) How hot will the greenhouse world be? *Science*, 309 (5731), 100. <https://doi.org/10.1126/science.309.5731.100>
- Kukal, Z. (1990) The rate of geological processes. *Earth-Science Reviews*, 28 (1-3), 73–82. [https://doi.org/10.1016/0012-8252\(90\)90017-P](https://doi.org/10.1016/0012-8252(90)90017-P)
- Kuroda, J., Ogawa, N.O., Tanimizu, M., Coffin, M.F., Tokuyama, H., Kitazato, H. & Ohkouchi, N. (2007) Contemporaneous massive subaerial volcanism and late cretaceous Oceanic Anoxic Event 2. *Earth and Planetary Science Letters*, 256 (1-2), 211–223. <https://doi.org/10.1016/j.epsl.2007.01.027>
- Lewis, S.L. & Maslin, M. A. (2015) Defining the Anthropocene. *Nature*, 519 (7542), 171–80. <https://doi.org/10.1038/nature14258>
- Li, Y.X., Bralower, T.J., Montañez, I.P., Osleger, D.A., Arthur, M.A., Bice, D.M., Herbert, T., Erba, E. & Silva, I.P. (2008) Toward an orbital chronology for the early Aptian oceanic anoxic event (OAE1a, ~120 Ma). *Earth and Planetary Science Letters*, 271 (1-4), 88–100. <https://doi.org/10.1016/j.epsl.2008.03.055>
- Li, Y. X., Montañez, I. P., Liu, Z. & Ma, L. (2017) Astronomical constraints on global carbon-cycle perturbation during Oceanic Anoxic Event 2 (OAE2). *Earth and Planetary Science Letters*, 462, 35–46. <https://doi.org/10.1016/j.epsl.2017.01.015>
- McInerney, F.A. & Wing, S.L. (2011) The Paleocene-Eocene Thermal Maximum: A perturbation of carbon cycle, climate, and biosphere with implications for the future. *Annual Review of Earth and Planetary Sciences*, 39 (1), 489–516. <https://doi.org/10.1146/annurev-earth-040610-133431>
- Menegatti, A.P., Weissert, H., Brown, R.S., Tyson, R.V., Farrimond, P., Strasser, A. & Caron, M. (1998) High-resolution  $\delta^{13}\text{C}$  stratigraphy through the early Aptian “Livello Selli” of the Alpine Tethys. *Paleoceanography*, 13 (5), 530–545. <https://doi.org/10.1029/98PA01793>
- Mutterlose, J., Bottini, C., Schouten, S. & Sinninghe Damsté, J.S. (2014) High sea-surface temperatures during the early Aptian Oceanic Anoxic Event 1a in the Boreal Realm. *Geology*, 42 (5), 439–442. <https://doi.org/10.1130/G35394.1>
- Naafs, B.D.A. & Pancost, R.D. (2016) Sea-surface temperature evolution across Aptian oceanic anoxic event 1a. *Geology*, 44 (11), 959–962. <https://doi.org/10.1130/G38575.1>
- Robinson, S.A., Heimhofer, U., Hesselbo, S.P. & Petrizzo, M.R. (2017) Mesozoic climates and oceans—a tribute to Hugh Jenkyns and Helmut Weissert. *Sedimentology*, 64 (1), 1–15. <https://doi.org/10.1111/sed.12349>
- Ruddiman, W.F., Ellis, E.C., Kaplan, J.O. & Fuller, D.Q. (2015) Defining the epoch we live in. *Science*, 348 (6230), 38–39. <https://doi.org/10.1126/science.aaa7297>
- Ruhl, M., Hesselbo, S.P., Al-Suwaidi, A., Jenkyns, H.C., Damborenea, S.E., Manceñido, M.O., Storm, M., Mather, T. & Riccardi, A.C. (2020) On the onset of Central Atlantic Magmatic Province (CAMP) volcanism and environmental and carbon-cycle change at the Triassic–Jurassic transition (Neuquén Basin, Argentina). *Earth-Science Reviews*, 208, 103229. <https://doi.org/10.1016/j.earscirev.2020.103229>
- Ruhl, M. & Kürschner, W.M. (2011) Multiple phases of carbon cycle disturbance from large igneous province formation at the Triassic–Jurassic transition. *Geology*, 39 (5), 431–434. <https://doi.org/10.1130/G31680.1>
- Ruhl, M., Veld, H. & Kürschner, W.M. (2010) Sedimentary organic matter characterization of the Triassic–Jurassic boundary GSSP at Kuhjoch (Austria). *Earth and Planetary Science Letters*, 292 (1-2), 17–26. <https://doi.org/10.1016/j.epsl.2010.01.020>
- Schaller, M.F., Wright, J.D. & Kent, D.V. (2011) Atmospheric  $\text{pCO}_2$  perturbations associated with the Central Atlantic Magmatic Province. *Science*, 331 (6023), 1404–1409. <https://doi.org/10.1126/science.1199011>
- Schneebeil-Hermann, E., Kürschner, W.M., Kerp, H., Bomfleur, B., Hochuli, P.A., Bucher, H., Ware, D. & Roohi, G. (2015) Vegetation history across the Permian–Triassic boundary in Pakistan (Amb section, Salt Range). *Gondwana Research*, 27 (3), 911–924. <https://doi.org/10.1016/j.gr.2013.11.007>
- Scott, R.W. (2016) Barremian–Aptian–Albian carbon isotope segments as chronostratigraphic signals: numerical age calibration and durations. *Stratigraphy*, 13 (1), 21–47. <https://doi.org/10.29041/strat.13.1.02>
- Shen, J., Zhang, Y.G., Yang, H., Xie, S. & Pearson, A. (2022) Early and late phases of the Permian–Triassic mass extinction

- marked by different atmospheric CO<sub>2</sub> regimes. *Nature Geoscience*, 15 (10), 839–844.  
<https://doi.org/10.1038/s41561-022-01034-w>
- Shen, S.Z., Zhang, F.F., Wang, W.Q., Fan, J., Chen, J., Wang, B., Cao, J., Yang, S., Zhang, H., Li, G., Deng, T., Li, X. & Chen, J. (2024) Deep-time major biological and climatic events versus global changes: Progresses and challenges. *China Science Bulletin*, 69, 268–285. [In English]  
<https://doi.org/10.1360/TB-2023-0218>
- Steffen, W., Grinevald, J., Crutzen, P. & McNeill, J. (2011) The Anthropocene: conceptual and historical perspectives. *Philosophical Transactions of the Royal Society A: Mathematical, Physical and Engineering Sciences*, 369 (1938), 842–867.  
<https://doi.org/10.1098/rsta.2010.0327>
- Suan, G., Pittet, B., Bour, I., Mattioli, E., Duarte, L.V. & Mailliot, S. (2008) Duration of the Early Toarcian carbon isotope excursion deduced from spectral analysis: consequence for its possible causes. *Earth and Planetary Science Letters*, 267 (3-4), 666–679.  
<https://doi.org/10.1016/j.epsl.2007.12.017>
- Sun, Y., Joachimski, M.M., Wignall, P.B., Yan, C., Chen, Y., Jiang, H., Wang, L. & Lai, X. (2012) Lethally hot temperatures during the Early Triassic greenhouse. *Science*, 338 (6105), 366–370.  
<https://doi.org/10.1126/science.1224126>
- Svensen, H. (2012) Bubbles from the deep. *Nature*, 483, 413–415.  
<https://doi.org/10.1038/483413a>
- Them II, T.R., Gill, B.C., Caruthers, A.H., Gröcke, D.R., Tulsky, E., Martindale, R.C., Poulton, T. & Smith, P.L. (2017) High-resolution carbon isotope records of the Toarcian Oceanic Anoxic Event (Early Jurassic) from North America and implications for the global drivers of the Toarcian carbon cycle. *Earth and Planetary Science Letters*, 459, 118–126.  
<https://doi.org/10.1016/j.epsl.2016.11.021>
- Tierney, J.E., Poulsen, C.J., Montañez, I.P., Bhattacharya, T., Feng, R., Ford, H.L., Hönisch, B., Inglis, G., Petersen, S., Sahoo, N., Tabor, C., Thirumalai, K., Zhu, J., Bruls, N., Foster, G., Godderis, Y., Huber, B., Ivany, L., Turner, S., Lunt, D., McElwain, J., Mills, B., Otto-Bliesner, B., Ridgwell, A. & Zhang, Y.G. (2020) Past climates inform our future. *Science*, 370 (6517), eaay3701.  
<https://doi.org/10.1126/science.aay3701>
- Wu, Y., Chu, D., Tong, J., Song, H., Dal Corso, J., Wignall, P.B., Song, H., Du, Y. & Cui, Y. (2021) Six-fold increase of atmospheric p CO<sub>2</sub> during the Permian–Triassic mass extinction. *Nature communications*, 12 (1), 2137.  
<https://doi.org/10.1038/s41467-021-22298-7>
- Zachos, J., Pagani, M., Sloan, L., Thomas, E. & Billups, K. (2001) Trends, rhythms, and aberrations in global climate 65 Ma to present. *Science*, 292 (5517), 686–693.  
<https://doi.org/10.1126/science.1059412>
- Zeebe, R.E., Ridgwell, A. & Zachos, J.C. (2016) Anthropogenic carbon release rate unprecedented during the past 66 million years. *Nature Geoscience*, 9 (4), 325–329.  
<https://doi.org/10.1038/ngeo2681>
- Zeebe, R.E., Zachos, J.C. & Dickens, G.R. (2009) Carbon dioxide forcing alone insufficient to explain Palaeocene–Eocene Thermal Maximum warming. *Nature Geoscience*, 2 (8), 576–580.  
<https://doi.org/10.1038/ngeo578>